Comparing chiral ferrocenyl and ruthenocenyl ligands: how subtle structural changes influence their performance in asymmetric catalysis

Comparing Chiral Ferrocenyl and Ruthenocenyl Ligands: How Subtle Structural Changes Influence Their Performance in Asymmetric Catalysis

Hendrikus C. L. Abbenhuis,[†] Urs Burckhardt,[†] Volker Gramlich,[‡] Arianna Martelletti,[‡] John Spencer,[†] Ivo Steiner,[†] and Antonio Togni*[,†]

Laboratory of Inorganic Chemistry and Institute of Crystallography and Petrography, Swiss Federal Institute of Technology, ETH-Zentrum, CH-8092 Zurich, Switzerland

Received November 21, 1995[⊗]

A route to enantiopure heteroleptic ruthenocenyl derivatives has been found; the diastereoselective addition of MeLi to (*R*)-CyCH(Me)N(Me)CH=C_5H_4 (de = 74%), followed by a transmetalation reaction with either $[Cp^*Ru(\mu^3\text{-}Cl)]_4$ or $[(p\text{-cymene})RuCl_2]_2/KPF_6$, afforded the heteroleptic complexes (*S*,*R*)-$[Cp^*Ru(\eta^5\text{-}C_5H_4CH(Me)N(Me)CH(Me)Cy)]$, **6**, or (*S*,*R*)-$[(p\text{-cymene})Ru(\eta^5\text{-}C_5H_4CH(Me)N(Me)CH(Me)Cy)]^+PF_6^-$, **5**, in 93% and 72% yields, respectively. Whereas **5** displayed a somewhat inert behavior, **6** reacted with $NHMe_2$, in acetic acid, to afford its dimethylamino congener (*S*)-**7** in 93% yield. The latter was converted in two steps into the bis(phosphine) derivatives (*S*)-(*R*)-$Cp^*RuC_5H_3CH(Me)PCy_2PPh_2$-2, (*S*)-(*R*)-**9**, and (*S*)-(*R*)-$Cp^*RuC_5H_3CH(Me)PC_8H_{14}PPh_2$-2, (*S*)-(*R*)-**10**, and into the P,N derivative (*S*)-(*R*)-$Cp^*RuC_5H_3CH(Me)\{N_2C_3HMe_2\text{-}3,5)PPh_2\}$-1,2, (*S*)-(*R*)-**11**. These products were obtained in >99% ee after recrystallization. The ruthenocenyl derivatives were probed for their use as chiral ligands for the palladium-catalyzed enantioselective allylic alkylation and the rhodium catalyzed hydroboration reactions. By employing the ruthenocenylpyrazole (*S*)-(*R*)-**11**, styrene was converted to (*S*)-1-phenylethanol with 87% ee, whereas its isostructural ferrocenyl congener (*S*)-(*R*)-**16** afforded 94% ee. The following compounds were characterized by X-ray diffraction: (*S*,*R*)-**5**, (*S*)-(*R*)-**9**, (*S*)-(*R*)-**10**, $[((S^*)\text{-}(R^*)\text{-}\mathbf{14})Pd(\eta^3\text{-}C_3H_5)]^+[OTf]^-$ ((*S**)-(*R**)-**12**), and $[((S^*)\text{-}(R^*)\text{-}\mathbf{9})Pd(\eta^3\text{-}C_3H_5)]^+[OTf]^-$ ((*S**)-(*R**)-**13**).

Introduction

By virtue of their high scope of application as ligands in a range of asymmetric reactions, optically active ferrocenyl phosphines,[1] exemplified by **1-3**, are becoming of increasing importance (see Chart 1).[2] The facile synthesis of a wide range of such derivatives, by a nucleophilic substitution reaction occurring with retention of configuration at the stereogenic center of the side chain, and the resulting structural diversity on the ferrocenyl unit, allow for a systematic study, and exploitation, of electronic and steric effects in enantioselective catalysis.[2e]

Chart 1

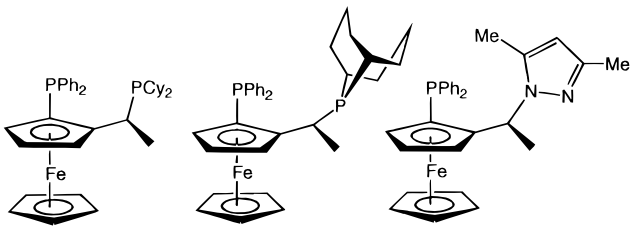

(*S*)-(*R*)-**1** (*S*)-(*R*)-**2** (*S*)-(*R*)-**3**

Recently, we reported a new stereoselective route to congeners of **1**−**3**, with the added advantage of allowing variation of the ("lower") nonfunctionalized Cp.[3] The key feature of the underlying synthetic strategy was to construct ferrocenes starting from enantiomerically enriched Cp synthons and a suitable iron(II) precursor. Hence, the synthesis of precursors to analogues of **1**−**3** was possible *via* a highly stereoselective addition of MeLi to one diastereotopic face of an enantiomerically pure fulvene derivative, followed by transmetalation with an iron(II) salt. The diastereoselectivity observed during the formation of one particular metalated cyclopentadienyl derivative (*S*,*R*)-**4** was as high as 87%. As a natural extension to this study, it was tempting to test whether this method was amenable for the synthesis of the corresponding heteroleptic ruthenocene complexes, namely by reaction of **4** with appropriate ruthenium(II) derivatives. This choice was potentially

[†] Laboratory of Inorganic Chemistry.
[‡] Institute of Crystallography and Petrography.
[⊗] Abstract published in *Advance ACS Abstracts,* February 15, 1996.

(1) For reviews, see: (a) Hayashi, T. In *Ferrocenes. Homogeneous Catalysis, Organic Synthesis, Materials Science*; Togni, A., Hayashi, T., Eds.; VCH: Weinheim, Germany, 1995; pp 105−142. (b) Sawamura, M.; Ito, Y. *Chem. Rev.* **1992**, *92*, 857−871. See also: (c) Hayashi, T.; Mise, T.; Fukushima, M.; Kagotani, M.; Nagashima, N.; Hamada, Y.; Matsumoto, A.; Kawakami, S.; Konishi, M.; Yamamoto, K.; Kumada, M. *Bull. Chem. Soc. Jpn.* **1980**, *53*, 1138−1151.

(2) For recent reports from our laboratories, see: (a) Togni, A.; Breutel, C.; Schnyder, A.; Spindler, F.; Landolt, H.; Tijani, A. *J. Am. Chem. Soc.* **1994**, *116*, 4062−4066. (b) Breutel, C.; Pregosin, P. S.; Salzmann, R.; Togni, A. *J. Am. Chem. Soc.* **1994**, *116*, 4067−4068. (c) Togni, A.; Breutel, C.; Soares, M. C.; Zanetti, N.; Gerfin, T.; Gramlich, V.; Spindler, F.; Rihs, G. *Inorg. Chim. Acta* **1994**, *222*, 213−224. (d) Abbenhuis, H. C. L.; Burckhardt, U.; Gramlich, V.; Köllner, C.; Pregosin, P. S.; Salzmann, R.; Togni, A. *Organometallics* **1995**, *14*, 759−766. (e) Schnyder, A.; Hintermann, L.; Togni, A. *Angew. Chem.* **1995**, *107*, 996−998 (*Angew. Chem. Int. Ed. Engl.* **1995**, *34*, 931−933). (f) Burckhardt, U.; Hintermann, L.; Schnyder, A.; Togni, A. *Organometallics* **1995**, *14*, 5415−5425. (g) Spencer, J.; Gramlich, V.; Häusel, R.; Togni, A. *Tetrahedron: Asymmetry* **1996**, *7*, 41−44. (h) Zanetti, N. C.; Spindler, F.; Spencer, J.; Togni, A.; Rihs, G. *Organometallics* **1996**, *15*, 860. (i) Togni, A.; Burckhardt, U.; Pregosin, P. S.; Salzmann, R. *J. Am. Chem. Soc.* **1996**, *118*, 1031−1037.

(3) Abbenhuis, H. C. L.; Burckhardt, U.; Gramlich, V.; Togni, A.; Albinati, A.; Müller, B. *Organometallics* **1994**, *13*, 4481−4493.

0276-7333/96/2315-1614$12.00/0

Scheme 1

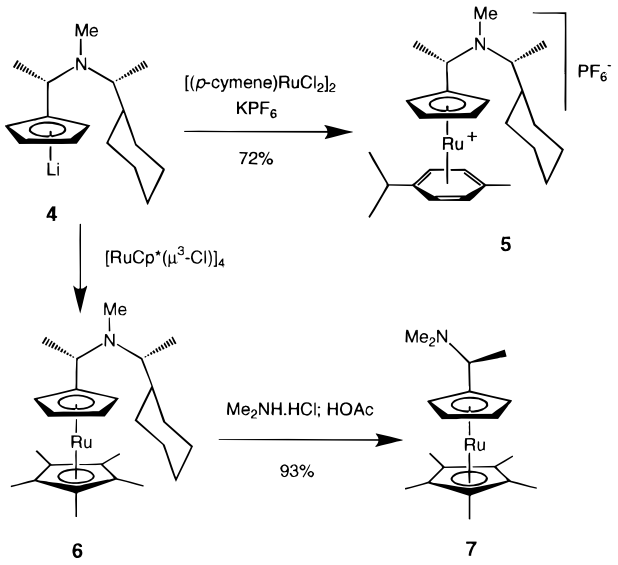

Scheme 2

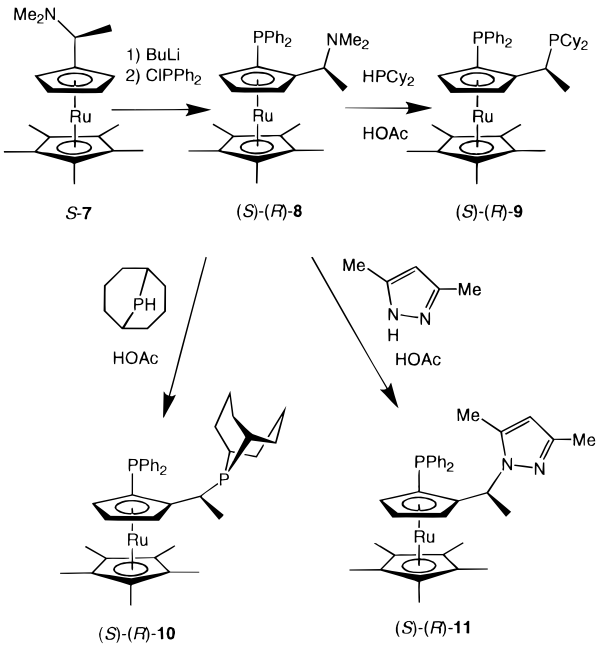

informative, as it would enable a direct comparison of structural and conformational aspects of similar Fe(II) and Ru(II) systems with a particular emphasis on their respective performances in catalysis.[4]

This account provides full synthetic details for the preparation of new enantiomerically enriched ruthenocenyl amines, as well as their derivatization to give new ligands for transition-metal-catalyzed asymmetric reactions. A comparison of the performance of such ligands with that of their isostructural ferrocenyl analogues is also presented.

Results and Discussion

Stereoselective Syntheses of Ruthenocenyl P,P and P,N Ligands. The "half-sandwich" complexes $[Cp^*Ru(\mu^3\text{-}Cl)]_4$[5] and $[(p\text{-cymene})RuCl_2]_2$[6] are convenient starting materials for the synthesis of the requisite heteroleptic Ru sandwich compounds. Transmetalations with the cyclopentadienyl synthon **4** proceed smoothly and afford respectively the cationic ruthenium amine derivative **5** and the neutral ruthenocenyl amine **6** (see Scheme 1). The latter is obtained in 93% yield as a dark oil after conventional workup involving its purification by flash chromatography over silica. The transmetalation of $[(p\text{-cymene})RuCl_2]_2$ with **4**, followed by an anion-exchange reaction with KPF_6, furnishes the cationic mixed sandwich derivative **5** in 72% yield as an air stable beige/brown solid. Since the cyclopentadienyl synthon (*S*,*R*)-**4** contains, due to the incomplete stereoselectivity in its formation (de = 74%), *ca.* 13% of the minor diastereoisomer (*R*, *R*)-**4**, the new heteroleptic complexes **5** and **6** should exist as approximate 7:1 mixtures of diastereoisomers. The ^1H and ^{13}C NMR resonances of the minor isomers, however, are not sufficiently dinstinguishable from those of the major diastereoisomers to allow an assessment of the diastereoisomeric purity of **5** or **6** by NMR. Gratifyingly, diastereoisomerically pure (*S*,*R*)-**5** can be easily obtained by crystallization from CH_2Cl_2/Et_2O mixtures. Moreover, the absolute configuration of **5** was elucidated by an X-ray structural analysis (vide infra). In the case of the ruthenocenyl amine **6**, which is invariably obtained as an oil, separation of the two diastereoisomers cannot be achieved by a simple crystallization procedure nor by column chromatography. This, however, does not hamper the obtention of virtually enantiomerically pure ruthenocenyl derivatives from **6** (*vide infra*).

Attempts to ortho-lithiate the ruthenocenyl derivatives **5** and **6** using *n*-BuLi were unsuccessful. As we recently reported for the related iron chemistry, this rather inert behavior toward ortho-metalation is ascribed to the presence of sterically demanding substituents at the nitrogen center, which may severely disfavor chelation in the lithiated ruthenocenyl intermediates. With the ruthenocenyl amine **6**, this complication can be easily alleviated since virtually quantitative conversion into its dimethylamino analogue **7** (see Scheme 1) is readily achieved. In contrast to the purification of **6**, which involves flash chromatography on silica, attempts to purify **7** by a similar procedure were unsuccessful and invariably led to decomposition of the compound to the vinyl complex, $Cp^*RuC_5H_4\text{-}CH{=}CH_2$. Subsequent lithiation of the ruthenocenyl amine **7** with *n*-BuLi occurs with high stereoselectivity, and the lithiated ruthenocene reacts readily with chlorodiphenylphosphine to give the enantiomerically enriched (diphenylphosphino)ruthenocenyl amine (*S*)-(*R*)-**8** (see Scheme 2) in nearly 70% yield. The diastereoselectivity of this reaction must be greater than 98%, as the (*S*)-(*S*)-diastereoisomer could never be identified. The analogous conversion of the cationic ruthenium amine **5** into its dimethylamine derivative could not be achieved. **5** is inert toward Me_2NH/HOAc at room temperature for 48 h or $Me_2NH{\cdot}HCl$/KOAc in HOAc at reflux temperature over similar periods of time. Such a lack of reactivity in this aminolysis reaction is probably due to the inability of the metal center to provide anchimeric assistance prior to solvolysis, as this would necessitate the generation of an unfavorable dicationic

(4) For a recent discussion of the differences between ruthenocenyl and ferrocenyl ligands. see: Hayashi, T.; Ohno, A.; Lu, S.; Matsumoto, Y.; Fukuyo, E.; Yanagi, K. *J. Am. Chem. Soc.* **1994**, *116*, 4221−4226 and references cited therein.

(5) Fagan, P. J.; Ward, M. D.; Calabrese, J. C. *J. Am. Chem. Soc.* **1989**, *111*, 1698−1719.

(6) Bennet, M. A.; Smith, A. *J. Chem. Soc., Dalton Trans.* **1974**, 233.

Table 1. Experimental Data for the X-ray Diffraction Study of (*S,R*)-5, (*S)-(*R**)-12, and (*S**)-(*R**)-13**

	compound		
	(*S,R*)-**5**	(*S**)-(*R**)-**12**	(*S**)-(*R**)-**13**
formula	$C_{26}H_{40}F_6NPRu$	$C_{45}H_{59}F_3FeO_3P_2PdS{\cdot}CH_2Cl_2$	$C_{45}H_{59}F_3O_3P_2PdRuS$
mol wt	612.6	961.24 + 84.93	1006.48
cryst dim (mm)	0.63 × 0.4 × 0.44	0.1 × 0.2 × 0.4	0.5 × 0.25 × 0.1
data coll *T* (°C)	20	20	20
cryst syst	orthorhombic	monoclinic	monoclinic
space goup	$P2_12_12_1$	$P2_1/c$	$P2_1/c$
a (Å)	10.575(6)	21.589(8)	23.78(7)
b (Å)	11.508(7)	13.825(5)	9.693(11)
c (Å)	23.221(14)	18.071(7)	20.83(3)
α (deg)		105.05(3)	110.7(2)
V (Å^3)	2826(3)	5209(3)	4490(15)
Z	4	4	4
ρ(calcd) (g·cm^{-3})	1.440	1.424	1.489
μ (cm^{-1})	6.66	9.78	9.05
F(000)	1264	2296	2064
diffractometer	Picker-STOE	STOE Picker	Syntex P21
radiation	Mo Kα (graphite monochrom), λ = 0.710 73 Å		
measd reflcns	$0 \le h \le 10$, $0 \le k \le 11$, $0 \le l \le 22$	$0 \le h \le 20$, $-13 \le k \le 0$, $-17 \le l \le 16$	$0 \le h \le 14$, $-7 \le k \le 7$, $-15 \le l \le 14$
2θ range (deg)	3.0−4.0.0	3.0−40.0	3.0−40.0
scan type	ω	ω	ω
scan width (deg)	1.00	1.00	1.05
bkgd time (s)	0.30 × scan time	0.25 × scan time	0.25 × scan time
max scan speed (deg·min^{-1})	1.0−4.0 in ω	1.0−4.0 in ω	1.0−4.0 in ω
no. of indep data coll	1535	4851	1739
no. of obsd reflcns (n_o)	1387 $\lvert F_o^2\rvert > 4.0\rho(\lvert F\rvert^2)$	3551 $\lvert F_o^2\rvert > 4.0\rho(\lvert F\rvert^2$	1475 $\lvert F_o^2\rvert > 4.0\rho(\lvert F\rvert^2)$
abs corr	N/A	N/A	face-indexed numerical
transm coeff			0.9079−0.9582
no. of params refined (n_v)	304	545	450
quantity minimized	$\sum w(F_o - F_c)^2$	$\sum w(F_o - F_c)^2$	$\sum w(F_o - F_c)^2$
weighting scheme	$w^{-1} = \sigma^2(F) + 0.0134F^2$	$w^{-1} = \sigma^2(F) + 0.0023F^2$	$w^{-1} = \sigma^2(F) + 0.0010F^2$
R[a]	0.0595	0.0657	0.0419
R_w[b]	0.0797	0.0926	0.0544
GOF[c]	0.75	1.64	1.70

[a] $R = \sum(\lvert\lvert F_o\rvert - (1/k)\lvert F_c\rvert\rvert)/\sum\lvert F_o\rvert$. [b] $R_w = \sum w(\lvert\lvert F_o\rvert - (1/k)\lvert F_c\rvert\rvert)^2/[\sum w\lvert F_o\rvert^2]^{1/2}$. [c] GOF = $[\sum w(\lvert F_o\rvert - (1/k)\lvert F_c\rvert)^2/(n_o - n_v)]^{1/2}$.

species. Consequently, we aborted further efforts to synthesize cationic ruthenocenyl phosphines from **5** and restricted the work presented herein on the use of (diphenylphosphino)ruthenocenyl amine (*S*)-(*R*)-**8**.

As with its iron analogue, the amine (*S*)-(*R*)-**8** can be easily obtained in highly enantiomerically enriched form (>99% ee) by selective crystallization of the racemate (*S**)-(*R**)-**8** from ethanol solutions of the enantiomerically enriched compound. It is important to note that the multistep synthesis of **8** from the chiral Cp synthon **4** is accompanied with no net loss of optical activity. This can be derived from analysis of the relative amounts of (*S**)-(*R**)-**8** and (*S*)-(*R*)-**8** which nicely mirror the diastereoselectivity observed during the generation of **4**. Subsequent derivatization of (*S*)-(*R*)-**8** by applying a series of standard transformations, all of which have precedence in the related ferrocenyl series,[3] enabled access to ligands (*S*)-(*R*)-**9**-**11** (see Scheme 2). The first member of this series, (*S*)-(*R*)-**9**, was obtained as yellow crystals in 62% yield, after chromatographic purification, by the substitution of the dimethylamino group of (*S*)-(*R*)-**8** with dicyclohexylphosphine in acetic acid. The phobyl (9-phospha[3.3.1]bicyclonon-9-yl) incorporating compound (*S*)-(*R*)-**10** was equally prepared from (*S*)-(*R*)-**8** as a yellow solid in 40% yield in an analogous manner using a technical mixture of phobane as phosphine source.[2d] The yellow solid (*S*)-(*R*)-**11** was synthesized from (*S*)-(*R*)-**8** using 3,5-dimethylpyrazole as nucleophile. Given that the diamagnetic shift reagent *R*-(−)-1-(9-anthryl)-2,2,2-trifluoroethanol was effective for the separation of the resonances of the racemic pyrazole ligand (*S**)-(*R**)-**11** by ^{1}H NMR, the ee of (*S*)-(*R*)-**11** was confirmed to be greater than 99%. The optical purity of the ligands (*S*)-(*R*)-**9** and **10** was checked by HPLC (see Experimental Section).

Solid State Structures of the Ruthenocenyl Derivatives (*S,R*)-5, (*S*)-(*R*)-9, and (*S*)-(*R*)-10. In order to establish the stereochemical integrity and to study conformational aspects, we carried out X-ray crystallographic studies on the new heteroleptic ruthenium sandwich derivatives (*S,R*)-**5**, (*S*)-(*R*)-**9**, and (*S*)-(*R*)-**10**. For comparative purposes it was especially indispensable to obtain data for the latter two ligands so as to assess the effect of a change in metal, from Fe to Ru, on, for example, the relative positions of the aryl groups of the diphenylphosphine fragment of the upper Cp ring and the flexibility of the metallocene unit as a whole. An ORTEP view of the first of this series, (*S,R*)-**5**, is shown in Figure 1, and Table 1 collects crystal data and refinement parameters. The ruthenium atom is embedded in a mixed sandwich comprising the η^6-bound *p*-cymene and η^5-bound Cp fragment derived from (*S,R*)-**4**. Bond lengths and angles turn out to be routine and compare with those of, e.g., the similar cationic mixed sandwich derivative $[Cp^*Ru(\eta^6\text{-}C_6(CH_3)_6)]^+$.[5] The present structural study proves the absolute configuration *S* at the C(6) stereogenic center, thus directly establishing the stereochemistry of the preferred diastereoisomer of cyclopentadienyl **4**.

Crystal data and ORTEP views of compounds **9** and **10** are provided as Supporting Information. The structure of derivative **9** can be compared to that of the

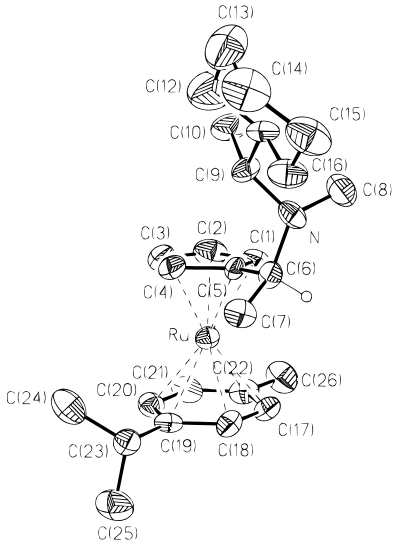

Figure 1. ORTEP view of the cation (*S*,*R*)-**5** (30% probability ellipsoids). The Ru atom is located at 1.831 Å from the Cp ring and 1.703 Å from the *p*-cymene ring. The planes of the two rings subtend an angle of 3.8°.

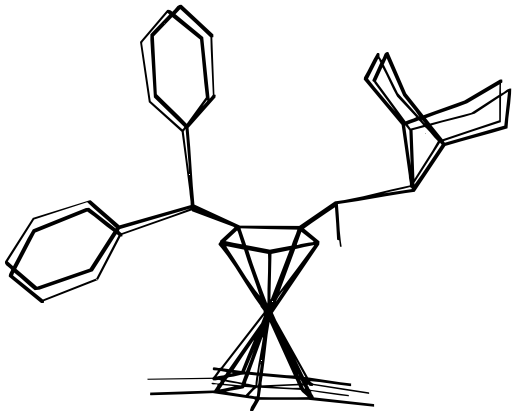

Figure 2. Schematic superposition of the structures of (*S*)-(*R*)-**10** and (*S*)-(*R*)-**15**,[3] showing the virtually identical conformation in the solid state.

corresponding Fe parent compound, Josiphos, **1**, reported recently from these laboratories.[2c] The only significant difference, besides the Ru-Cp (vs Fe−Cp) distances, pertains to the relative orientation of the cyclohexyl rings, indicating that the PCy_2 group constitutes the conformationally most flexible part of the molecule. The structural features of compound **10** are, not surprisingly, virtually identical to those of the corresponding Fe derivative **15** (see Chart 2), discussed in detail previously.[3] The only obvious difference is the increased Cp−Cp* distance in **10** (Ru−Cp 1.824 Å and Ru−Cp* 1.808 Å), as compared to **15**. The similarity of derivative **10** with its Fe congener is illustrated in the schematic superposition of the two structures given as Figure 2.

On the basis of the conformational characteristics observed for the free ligands **9** and **10**, as compared with similar Fe derivatives, one would anticipate no important differences between the Ru- and Fe-containing ligands, respectively, in their coordination behavior and hence in the catalytic performances of their complexes. As we will discuss below, this conclusion turns out to be incorrect, because of further unexpected features of the complexes containing the heavier element Ru.

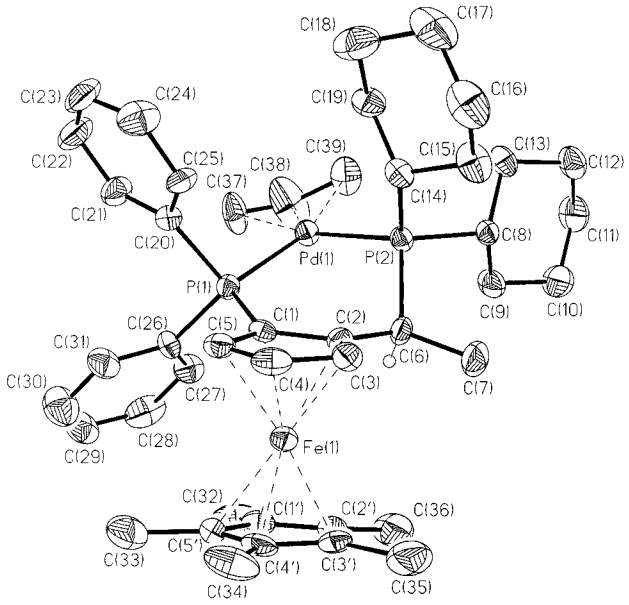

Figure 3. ORTEP view of the cation (*S**)-(*R**)-**12** (30% probability ellipsoids).

Structural Comparison of Palladium η^3-Allyl Complexes Incorporating Ruthenocenyl and Ferrocenyl Phosphines. Having established a marked similarity of the structural/conformational attributes of the Ru-containing ligands, when compared to the corresponding Fe derivatives, it was now necessary to compare the two systems as ligands. We opted for the facile synthesis and structural characterization of their cationic palladium η^3-allyl complexes, following procedures already employed in our laboratory.[2d] The racemic ruthenocene (*S**)-(*R**)-**9** and its isostructural bis(phosphine) iron analogue (*S**)-(*R**)-**14** were chosen as ligands (eq 1).

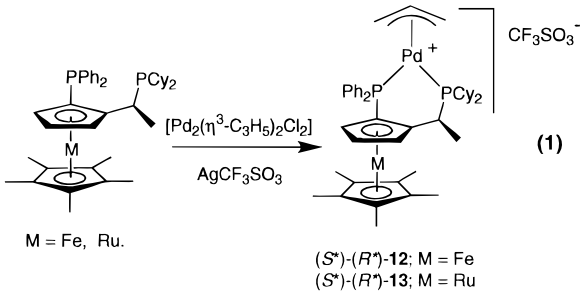

The single-crystal X-ray structures of the resulting palladium η^3-allyl complexes (*S**)-(*R**)-**12** and (*S**)-(*R**)-**13** were consequently determined. Their ORTEP views are shown in Figures 3 and 4, respectively. Crystal and refinement parameters are given in Table 1, and Table 2 collects pertinent bond lengths and angles, and torsion angles for both compounds.

Again, for the sake of simplicity, it is appropriate to compare the structure of complex **12** with that of the known compound containing the nonmethylated ligand Josiphos (**1**).[2c] The superposition of the two structures, shown in Figure 5, indicates a strong similarity of the conformational features. At first sight, the only relevant effect due to the addition of five 1′−5′ methyl groups in **12** is shown by the relative position and orientation of the PPh_2 group. It turns out that the latter is "pushed up" even more than in the parent compound. This is

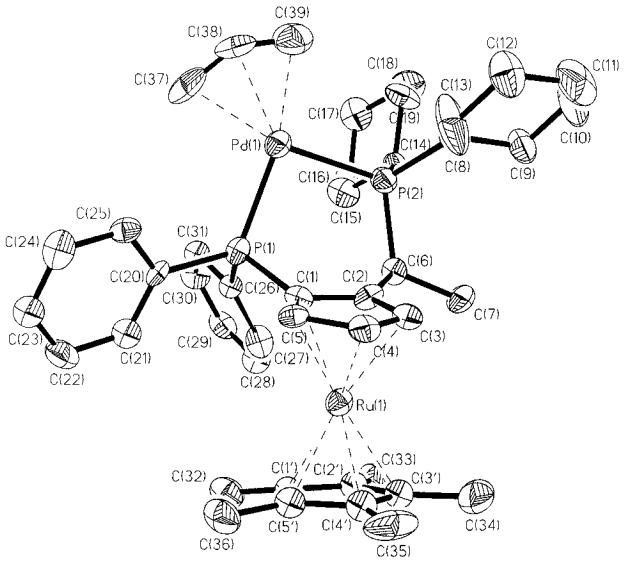

Figure 4. ORTEP view of the cation (*S**)-(*R**)-**13** (30% probability ellipsoids).

Table 2. Selected Bond Distances (Å),[a] Angles (deg),[a] and Torsion Angles (deg) for (S*)-(R*)-12 and (S*)-(R*)-13

	(S*)-(R*)-**12**	(R*)-(S*)-**13**
	Bond Distances	
Pd−P(1)	2.295(3)	2.285(8)
Pd−P(2)	2.312(3)	2.353(8)
Pd−C(37)	2.207(15)	2.163(27)
Pd−C(38)	2.129(20)	2.108(35)
Pd−C(39)	2.180(13)	2.118(25)
M−Cp*	1.678	1.805
M−Cp	1.661	1.819
	Bond Angles	
P(1)−Pd−P(2)	95.3(1)	94.0(2)
P(1)−Pd−C(37)	95.2(4)	100.3(6)
P(2)−Pd−C(39)	102.8(4)	99.3(7)
Pd−P(1)−C(1)	116.6(4)	106.2(6)
Pd−P(2)−C(6)	106.3(3)	112.4(6)
C(37)−C(38)−C(39)	141.4(23)	148.7(36)
Cp−Cp*	9.0	12.6
	Torsion Angles	
Pd−P(1)−C(1)−C(2)	8	53
Pd−P(2)−C(6)−C(2)	73	48
P(1)−C(1)−C(5)−C(4)	162	158
C(4)−C(3)−C(2)−C(6)	180	167
P(2)−C(6)−C(2)−C(1)	62	68

[a] Numbers in parentheses are esd's in the least significant digits.

clearly because of severe nonbonding interactions between the protruding Cp* ligand and the C(26)-C(31) phenyl group, as illustrated by (1) the short distance between the plane defined by the latter and the methyl group C(32) of 3.33 Å (shortest atom to atom separation is C(28)−C(32) of 3.53 Å), (2) the Cp−Cp* angle of 9°, and (3) the out-of-plane position of the phosphorus atom P(1). Its distance from the plane of the "upper" Cp ring is now 0.49 Å (vs 0.29 Å for the parent compound). Whereas in the Josiphos-containing complex one could describe the two phenyl groups in terms of axial and equatorial positions for the "lower" and the "upper" aryl, respectively, this distinction no longer applies to **12**. Both substituents on P(1) assume pseudo-equatorial positions. The conformation of the rest of the molecule is very similar in both compounds. Finally, from a qualitative point of view, the overall conformation of the Fe-containing ligand **14** in the Pd−allyl complex **12** matches very well the one of the free parent ligand Josiphos. On the basis of these considerations only, one is tempted to assume that the replacement of the unsubstituted Cp by Cp*, and, by extension, even more so the introduction of Ru instead of Fe, would not have very significant consequences on the conformational properties of the respective complexes. Therefore, if ground-state conformational considerations on complexes are important in the discussion of the catalytic performance of the different ligands, it could be anticipated that the three ligands Josiphos, **9**, and **14** should behave in a comparable manner.

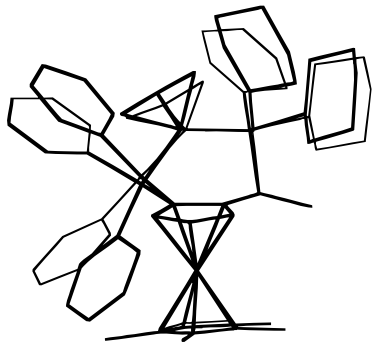

Figure 5. Schematic superposition of the structures of the cation (*S**)-(*R*")-**12** and the corresponding complex containing the ligand Josiphos (**1**),[2c] showing the very similar conformation in the solid state.

The structure of the Ru derivative **13**, however, shows some unusual and unexpected features. First of all, the orientation of the Pd−allyl fragment turns out to be completely different from that found in the analogous complex **12**. The Pd atom seems to adopt the most remote position from the ruthenocene core. This is illustrated by the large angle subtended by the planes of the Cp ring and the one defined by the atoms Pd, P(1), and P(2) of 76° (vs 22.5° for the corresponding angle in **12**). The most astonishing related feature is the orientation of the two Ph groups on P(1). Both are in a pseudo-equatorial position, pointing "down", i.e. toward the Cp*Ru fragment. The steric repulsion between the Ph groups and the Cp* ligand (shortest nonbonding distance is 3.47 Å for C(27)−C(32)) is relieved by the severe distortion around C(1), with P(1) located 0.56 Å above the Cp plane. This distortion is in part also transmitted to C(2), with C(6) positioned at 0.25 Å (vs 0.01 Å in **12**) from the same plane. These features seem to indicate an enhanced deformability of the ruthenocene core, as compared to ferrocene, in this class of compounds. A tentative conclusion from these observations is that complexes containing ruthenocenyl ligands will be conformationally more flexible than their ferrocenyl counterparts.

Asymmetric Catalysis Involving the Ruthenocenyl Derivatives *(S)*-(*R*)-9−11 as Ligands. Carrying on from our very successful exploitation of ligands **1**−**3** in a wide range of asymmetric processes, often giving rise to ee's well in excess of 90%, a few catalytic applications of the new ruthenocenes *(S)*-(*R*)-**9**−**11** were attempted. Two routine reactions were performed, viz. the palladium-catalyzed alkylation of 1,3-diphenyl-3-acetoxypropene with dimethyl malonate (see Table 3),[7] and the rhodium-catalyzed hydroboration of styrene (see Table 4).[8] As a comparison, the recently introduced

Table 3. Palladium-Catalyzed Alkylation of 1,3-Diphenyl-3-Acetoxypropene with Dimethyl Malonate[a]

entry	ligand	time (h)	conversion (%)	% ee (abs conf)
1	(*S*)-(*R*)-**9**	0.5	53	77 (*R*)
2	(*S*)-(*R*)-**9**	36	100	73 (*R*)
3	(*S*)-(*R*)-**14**	0.75	15	78 (*R*)
4	(*S*)-(*R*)-**14**	50	28	77 (*R*)
5	(*S*)-(*R*)-**10**	44	22	21 (*S*)
6	(*S*)-(*R*)-**10**	92	26	18 (*S*)
7	(*S*)-(*R*)-**11**	44	10	28 (*S*)
8	(*S*)-(*R*)-**11**	96	100	27 (*S*)

[a] Catalytic experiments were carried out as described in ref 2a using 1.0 mol % of catalyst at 20 °C.

Table 4. Rhodium-Catalyzed Hydroboration of Styrene[a]

entry	ligand	*T* (°C)	time (h)	regio-selectivity	% ee (abs conf)
1	(*S*)-(*R*)-**9**	20	7	95	40 (*S*)
2	(*S*)-(*R*)-**9**	0	7	99	37 (*S*)
3	(*S*)-(*R*)-**14**	20	18	95	54 (*S*)
4	(*S*)-(*R*)-**10**	20	7	89	34 (*S*)
5	(*S*)-(*R*)-**10**	0	7	88	26 (*S*)
6	(*S*)-(*R*)-**15**	20	18	77	32 (*S*)
7	(*S*)-(*R*)-**11**	20	18	67	87 (*R*)
8	(*S*)-(*R*)-**16**	20	18	76	94 (*R*)
9	(*S*)-(*R*)-**16**	0	18	68	92 (*R*)

[a] Catalytic experiments were carried out as described in ref 2a using 1.0 mol % of catalyst. Complete conversion of the starting material styrene was achieved in all cases listed here. Regioselectivity refers to % of 1-phenylethanol.

Chart 2

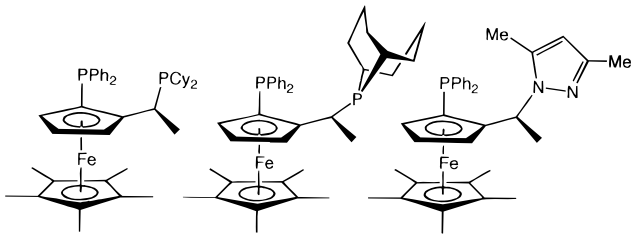

isostructural ferrocenyl derivatives *(S)*-(*R*)-**14**−**16** were also tested (see Chart 2).

From Table 3, a few important conclusions can be drawn. It is apparent that the activities of the catalysts are rather low; quantitative conversion of the allylic substrate when employing compounds *(S)*-(*R*)-**9** and *(S)*-(*R*)-**11** is only achieved after 36 and 96 h, respectively (entries 2 and 8, Table 3). For the other catalysts employed low conversions were observed even after as much as 92 h. The enantioselectivities observed for these reactions are equally rather low, reaching a maximum of 78%, after 0.75 h of reaction, for the ferrocenyl ligand *(S)*-(*R*)-**14**, although the activity of this catalyst is hampered by its low stability and rapid deactivation; even after 50 h only 28% conversion is attained. It is pertinent to note that the nonmethylated parent ligand **1** gave 93% ee and 99% yield for the same reaction after only 3 h. For the ruthenocenyl ligands employed in these tests very disappointing ee's and activities were observed, *(S)*-(*R*)-**10** and *(S)*-(*R*)-**11** giving ee's much lower than 30%, and the opposite enantiomer was obtained in each case. As with the ferrocene *(S)*-(*R*)-**14**, these reactions (entries 5−8) suffered from catalyst deactivation over prolonged periods.

The rhodium-catalyzed hydroboration of styrene continues to be an active subject of research in ours and other laboratories.[2e,8] Our results obtained with the new ligands presented in Table 4 show certain useful trends. Once again, the incorporation of a Cp* fragment into the ferrocenyl ligand *(S)*-(*R*)-**14** has a detrimental effect on the enantioselectivity. Thus, whereas *(R)*-(*S*)-**1** is an extremely useful ligand for this reaction (91.5% ee at −78°C), *(S)*-(*R*)-**14** is rather disappointing (54% ee, entry 3, Table 4), as is the corresponding ruthenocene, *(S)*-(*R*)-**9** (40% ee). In line with our previously reported observations, the best results are obtained with ligands incorporating pyrazole functions, although in these cases the regioselectivity of the reaction is rather low. Thus, the ruthenocenyl derivative *(S)*-(*R*)-**11** as ligand yields *(S)*-1-phenylethanol with an ee of 87% and 67% regioselectivity, whereas the ferrocenyl derivative *(S)*-(*R*)-**16** yields the same alcohol with an ee of 94% accompanied with a significantly higher regioselectivity (76%) (entries 7 and 8). The highest regio and enantioselectivities were attained with the latter ligand at 20 °C.

Conclusions

Hayashi *et al.* recently reported an improvement in the enantioselectivity of a number of palladium-catalyzed allylic substitution reactions on moving from a ferrocenyl to a ruthenocenyl bis(phosphine) system, whereby one phosphino fragment was situated on the upper and the other on the lower Cp ring.[4] Here, the greater distance between the cyclopentadienyl rings in the ruthenocene system leads to a larger bite angle. This was postulated to engender a tighter arrangement of the substituents on the phosphorus atoms, thus creating a more rigid "chiral pocket". Our system is significantly different from the latter in that in our case the two chelating fragments, viz. PP or PN functions, are located on the same, upper cyclopentadienyl ring. The unexpected structural features of complex **13** are interpreted as an expression of the greater conformational flexibility associated with our ruthenocenyl system, translating into a less efficient transmission of the chiral information in the catalytic reactions. In the Cp* ferrocene system, the larger lower ring seems to be responsible for a general decrease in activity in the Pd-catalyzed allylic chemistry, probably because of a much slower oxidative addition of the substrate, caused by unfavorable steric interactions. On the other hand, the Cp* ligand does not have any detrimental effects in the Rh-

(7) For reviews, see: (a) Consiglio, G.; Waymouth, R. M. *Chem. Rev.* **1989**, *89*, 257−276. (b) Hayashi, T. In *Catalytic Asymmetric Synthesis*; Ojima, I., Ed.; VCH: New York, 1993; pp 325−365. (c) Godleski, S. A. In *Comprehensive Organic Synthesis*; Trost, B. M., Fleming, I., Eds.; Pergamon: Oxford, U.K., 1991; Vol. 4, Chapter 3.3, pp 585−661. (d) Frost, C. G.; Howarth, J.; Williams, J. M. J. *Tetrahedron: Asymmetry* **1992**, *3*, 1089−1122. For a recent example, see: (e) von Matt, P.; Lloyd-Jones, G. C.; Minidis, A. B. E.; Pfaltz, A.; Macko, L.; Neuburger, M.; Zehnder, M.; Rüegger, H.; Pregosin, P. S. *Helv. Chim. Acta* **1995**, *78*, 265−284 and references cited therein.

(8) For a recent review, see: (a) Burgess, K.; Ohlmeyer, M. J. in *Homogeneous Transition Metal Catalyzed Reactions* (*Adv. Chem. Ser. 230*); (Moser, W. R., Slocum, D. W., Eds.; American Chemical Society: Washington, DC, **1992**; pp 163−177 and references cited therein. For specific examples, see: (b) Hayashi, T.; Matsumoto, Y.; Ito, Y. *J. Am. Chem. Soc.* **1989**, *111*, 3426−3428. (c) Matsumoto, Y.; Hayashi, T. *Tetrahedron Lett.* **1991**, *32*, 3387−3390. (d) Hayashi, T.; Matsumoto, Y.; Ito, Y. *Tetrahedron: Asymmetry* **1991**, *2*, 601−612. (e) Burgess, K.; van der Donk, W. A.; Ohlmeyer, M. J. *Tetrahedron: Asymmetry* **1991**, *2*, 613−621. (f) Brown, J. M.; Hulmes, D. I.; Layzell, T. P. *J. Chem. Soc., Chem. Commun.***1993**, 1673−1674.

catalyzed hydroboration of styrene, and indeed ligand **16** gives virtually identical results as its nonmethylated congener.[1e] We interpret this result as indicative of very similar structural/conformational properties of the two catalytically active complexes, not being influenced by the steric nature of the lower Cp ring.

The present work has shown that structural variations in peripheral regions of metallocene ligands may change their catalytic properties in a drastic manner. We demonstrated that (1) the introduction of a Cp* fragment in our ferrocenyl ligands, instead of a nonsubstituted cyclopentadienyl, and (2) the replacement of Fe by Ru, respectively, has different consequences on their catalytic performances. For diphosphine derivatives forming six-membered chelate rings, both changes have detrimental effects. In the case of the pyrazole-containing derivatives forming seven-membered chelates, the influence of both the Cp* and ruthenium is much less pronounced.

Experimental Section

General Considerations. All reactions with air- or moisture-sensitive materials were carried out under Ar using standard Schlenk techniques. Freshly distilled, dry, and oxygen-free solvents were used throughout. Technical grade phobane was obtained by courtesy of Prof. A. Salzer, RWTH Aachen, and was used as received. Routine ^{1}H (250.133 MHz), ^{13}C (62.90 MHz), and ^{31}P (101.26 MHz) spectra were recorded with a Bruker AC 250 spectrometer. Chemical shifts are given in ppm and coupling constants (J) are given in hertz. Merck silica gel 60 (70−230 mesh) was used for column chromatography. Optical rotations were measured with a Perkin-Elmer 341 polarimeter using 10 cm cells. Elemental analysis were performed by the "Mikroelementar-analytisches Laboratorium der ETH". Catalytic experiments and analysis of reaction products were carried out as previously described.[2a]

(*S,R*)-[(*p*-cymene)Ru(C_5H_4CH(Me)N(Me)CH(Me)Cy)]$^+$-[PF_6]$^-$ ((*S,R*)-5). A cooled THF solution (−40 °C) of LiC_5H_4-CH(Me)N(Me)CH(Me)Cy (freshly prepared from 0.82 g (3.8 mmol) of (*R*)-C_5H_4═CHN(Me)CH(Me)Cy and 2.4 mL of 1.6 M MeLi (3.8 mmol) at 0 °C) was transferred *via* cannula to a THF (15 mL) suspension of [(*p*-cymene)$RuCl_2$]$_2$ (1.1 g, 1.9 mmol) that was also kept at −40 °C. After being warmed up to room temperature and stirred for 1.5 h, the resulting red solution was filtered and the filtrate evaporated *in vacuo*. To the resulting red oil was added MeOH (50 mL) and excess KPF_6 (1.3 g, 7.1 mmol). After 1 h of stirring at room temperature, evaporation of the solvent afforded a brown solid that was subsequently extracted with CH_2Cl_2 (3 × 70 mL), filtered to remove impurities and excess inorganic salts, and concentrated *in vacuo* to ca. 10 mL. Addition of Et_2O (60 mL) induced precipitation of 1.7 g (72%) of brown product ($[\alpha]_D^{20}$ = 7.6 (CH_2Cl_2, c = 0.1)). ^{1}H NMR (250 MHz, $CDCl_3$): δ 6.01 (m, 4H, Ar), 5.32 (s, 1H, C_5H_4), 5.22 (m, 3H, C_5H_4), 3.51 (q, 1H, ^3J(H,H) = 6.8, CHMe), 2.68 (q, 1H, $CHMe_2$, ^3J(H,H) = 6.8), 2.32 (m, 3H, Me), 2.02 (s, 3H, Me), 1.69 (m, 3H, NMe), 1.24 (d, 6H, Me_2CH, ^3J(H,H) = 6.8), 1.91−0.75 (m, 11H, Cy). ^{13}C NMR (63 MHz, $CDCl_3$): δ 136.0, 117.6, 87.1, 86.8, 84.5, 84.4, 80.7 (C_5H_4 and Ar), 59.8, 55.9 (CHMeN), 42.0 (NMe), 32.0, 31.0, 30.7, 29.9, 26.6, 26.5 (Cy), 23.4 ($CHMe_2$), 19.7 ($CHMe_2$), 16.4, 13.5 (CHMeN). MS (FAB) (*m/e*) 468 (M^+, 100%). Anal. Calcd for $C_{26}H_{40}NF_6PRu\cdot CH_2Cl_2$: C, 46.49; H, 6.07; N, 2.01. Found: C, 46.74; H, 6.03; N, 2.00.

(*S,R*)-Cp*RuC_5H_4CH(Me)N(Me)CH(Me)Cy ((*S,R*)-6). To a solution of LiC_5H_4CH(Me)N(Me)CH(Me)Cy in ca. 30 mL of THF (prepared from 4.4 g (20 mmol) of (*R*)-C_5H_4═CHN(Me)-CH(Me)Cy and 13 mL of 1.6 M MeLi (21 mmol) at 0 °C) was added [Cp*Ru(μ^3-Cl)]$_4$ (5.0 g, 4.6 mmol). The resulting dark-brown solution was stirred for 30 min. Water (150 mL) was added and the water layer extracted with hexane (3 × 200 mL). The combined extracts were dried over $MgSO_4$ followed by removal of the solvent *in vacuo*. The residual brown oil was purified by chromatography on silica using hexane (containing ca. 5% of Et_3N). Yield: 8.0 g (93%) of dark oil. ^{1}H NMR (250 MHz, $CDCl_3$): δ 4.1 (m, 4H, C_5H_4), 3.35 and 2.38 (both q, 2 × 1H, CH(Me)N), 2.1 (s, 3H, NMe), 1.9 (s, 15H, C_5Me_5), 1.17 and 0.75 (both d, 2 × 3H, CHMeN). ^{13}C NMR (63 MHz, $CDCl_3$): δ 93.4 (ipso-C of C_5H_4), 84.4 (ipso-C of C_5Me_5), 73.4, 72.6, 71.8, 70.9 (C_5H_4), 58.4 (CpCH), 56.5 (CpCHMeNMeCH), 42.2 (NMe), 31.1−26.7 (Cy), 15.4 and 13.4 (both CHMeN), 11.8 (C_5Me_5). Anal. Calcd for $C_{26}H_{41}NRu$: C, 66.63; H, 8.82; N, 2.99. Found: C, 66.79; H, 8.63; N, 2.88.

(*S*)-Cp*RuC_5H_4CH(Me)NMe_2 ((*S*)-7). To a cooled (ca. −10 °C) dark solution of (*S,R*)-**6** (13.8 g, 29.3 mmol) in $HNMe_2$ (25 mL) was slowly added 45 mL of AcOH. The resulting solid was heated for 30 min at 60 °C, giving a clear dark solution. Water (ca. 100 mL) was added and the pH adjusted to ca. 10 by careful addition of NaOH. Extraction with hexane (3 × 200 mL), followed by drying of the combined extracts over $MgSO_4$ and removal of the solvent *in vacuo*, gave a dark oil that contained the product together with HN(Me)CH(Me)Cy. This *sec*-amine was distilled off (100 °C, 0.1 Torr) leaving the product as a brown oil; yield 10.2 g (93%). ^{1}H NMR (250 MHz, $CDCl_3$): δ 4.1 (m, 4H, C_5H_4), 3.24 (q, 1H, CHMe), 2.1 (s, 6H, NMe_2), 1.9 (s, 15H, C_5Me_5), 1.23 (d, 3H, CHMe). ^{13}C NMR (63 MHz, $CDCl_3$): δ 89.5 (ipso-C of C_5H_4), 84.1 (ipso-C of C_5Me_5), 73.2, 72.2, 71.8, 70.4 (C_5H_4), 57.5 (CpCH), 40.4 (NMe_2), 14.6 (CHMeN), 11.6 (C_5Me_5). Anal. Calcd for $C_{19}H_{29}NRu$: C, 61.26; H, 7.85: N, 3.76. Found: C, 61.74; H, 7.68; N, 3.40.

(*S*)-(*R*)-Cp*RuC_5H_3CH(Me)NMe_2PPh_2-2 ((*S*)-(*R*)-8). A solution of (*S*)-**7** (10.2 g, 27.4 mmol) and BuLi (19 mL 1.6 M (30.4 mmol in hexane) in Et_2O (50 mL) was stirred for 2 days. Subsequently, PPh_2Cl (6.0 mL, 32 mmol) was added and the resulting brown suspension was refluxed for 4 h followed by careful addition of saturated $NaHCO_3$ (ca. 30 mL). Extraction with toluene (3 × 100 mL) followed by drying of the combined organic layers on $MgSO_4$ and removal of the solvent in vacuo gave a reddish oil. This was subjected to flash chromatography over silica using hexane (containing ca. 5% of Et_3N) in order to elute impurities followed by elution of the product with THF. Finally, the product was purified by flash chromatography over Al_2O_3 using toluene (containing ca. 5% of Et_3N) affording 10.2 g (67%) of product. Crystallization from ethanol gave 1.7 g of crystalline, pale yellow, almost racemic product ($[\alpha]_D^{20}$ = 14 ($CHCl_3$, c = 1.0)) while removal of the solvent from the mother liquor in vacuo left 8.5 g of almost optically pure compound as a red oil ($[\alpha]_D^{20}$ = 248 ($CHCl_3$, c = 0.44)). ^{1}H NMR (250 MHz, $CDCl_3$): δ 7.62 (m, 2H, PPh_2), 7.27 (m, 8H, PPh_2), 4.23 (m, 3H, C_5H_3), 3.65 (dq, 1H, CHMeN, ^3J(H,H) = 6.5, ^4J(P,H) = 1.7), 1.90 (s, 15H, C_5Me_5), 1.78 (s, 6H, NMe_2), 0.98 (d, 3H, CH(Me)N). ^{13}C NMR (63 MHz, $CDCl_3$): δ 135.0−126.8 (non quartenary C of PPh_2), 85.1 (C_5Me_5), 75.9, 74.8, 74.0 (non quartenary C of C_5H_3), 56.1 (CHMeN), 38.4 (NMe_2), 11.5 (C_5Me_5), 7.2 (CHMeN). ^{31}P NMR (101 MHz, $CDCl_3$): δ −24.6 (s, PPh_2). Anal. Calcd for $C_{31}H_{38}NPRu$: C, 66.88; H, 6.88: N, 2.52. Found: C, 66.95; H, 6.88; N, 2.47.

(*S*)-(*R*)-Cp*RuC_5H_3CH(Me)PCy_2PPh_2-2 ((*S*)-(*R*)-9). A solution of (*S*)-(*R*)-**8** (0.95 g, 1.7 mmol) and $HPCy_2$ (0.38 mL, 1.9 mmol) in AcOH (35 mL) was stirred at 80 °C for 2 h. The solvent was removed *in vacuo* and the sticky residue subjected to flash chromatography on Al_2O_3 using hexane/toluene (3:1, containing 5% Et_3N) as eluent. The product was obtained analytically pure after crystallization from a minimum of hot EtOH; yield 0.75 g (62%) of pale yellow crystals ($[\alpha]_D^{20}$ = 253 ($CHCl_3$, c = 1.1)). Note: the racemic compound (prepared *via* the same method from racemic Cp*RuC_5H_3CH(Me)NMe_2PPh_2-2) can be separated on a Daicel Chiracel OD-H column (hexane/2-propanol = 99.5:0.5, flow = 1.0 mL·min^{-1}) with R_t (*R*)-(*S*) = 3.34 min and R_t (*S*)-(*R*) = 3.44 min. ^{1}H NMR (250 MHz, $CDCl_3$): δ 7.63 (m, 2H, PPh_2), 7.25 (m, 8H, PPh_2), 4.44, 4.13 (m, 3H, C_5H_3), 2.79 (dq, 1H, CHMeP, ^3J(H,H) = 5.4,

J(P,H) = 2.2 Hz), 1.73 (s, 15H, C_5Me_5), 1.38 (dd, 3H, CHMeP, ^3J(H,H) = 5.7, ^3J(H,P) = 7.1), 1.8−1.3 (m, 22H, Cy). ^{13}C NMR (63 MHz, $CDCl_3$): δ 135.7−126.7 (nonquartenary C of PPh_2), 85.0 (C_5Me_5), 75.6, 74.5, 74.1 (nonquartenary C of C_5H_5), 32.7−24.7 (PCy_2), 18.2 (CHMeP), 11.6 (C_5Me_5). ^{31}P NMR (101 MHz, $CDCl_3$): δ −26.3 (d, PPh_2, ^4J(P,P) = 36 Hz), 11.5 (d, PCy_2, ^4J(P,P) = 36 Hz). Anal. Calcd for $C_{41}H_{54}P_2Ru$: C, 69.37; H, 7.67. Found: C, 69.62; H, 7.62.

(*S*)-(*R*)-Cp*RuC$_5$H$_3$CH(Me)PC$_8$H$_{14}$PPh$_2$-2 ((*S*)-(*R*)-10). The procedure is the same as that for (*S*)-(*R*)-**9** except that *(S)*-(*R*)-**8** (0.40 g, 0.72 mmol) and HPC_8H_{14} (1.28 g, 8.8 mmol, 2:1 mixture of [3.3.1] and [4.2.1] isomers) reacted to give 0.19 g (40%) of pale yellow crystalline product ($[\alpha]_D^{20}$ = +182, ($CHCl_3$, c = 0.70)). Note: the racemic compound (prepared via the same method from racemic Cp*RuC$_5$H$_3$CH(Me)NMe$_2$-PPh$_2$-2) can be separated on a Daicel Chiracel OD-H column (hexane/2-propanol = 99.0:1.0, flow = 0.5 mL·min^{-1}) with R_t *(R)-(S)* = 7.19 min and R_t *(S)-(R)* = 7.44 min. ^{1}H NMR (250 MHz, $CDCl_3$): δ 7.58 (m, 2H, PPh_2), 7.26 (m, 8H, PPh_2), 4.65, 4.10, and 4.06 (m, 3H, C_5H_3), 2.80 (q, 1H, CHMeP, ^3J(H,H) = 6.2), 1.76 (s, 15H, C_5Me_5), 2.0−1.0 (m, 14H, C_8H_{14}), 1.40 (dd, 3H, CHMeP, ^3J(H,H) = 6.2, ^3J(H,P) = 13). ^{13}C NMR (63 MHz, $CDCl_3$): δ 140.8−127.8 (nonquartenary C of PPh_2), 85.7 (C_5Me_5), 75.2, 75.4, 73.8 (non quartenary C of C_5H_3), 32.4−23.3 (PC_8H_{14}), 21.5 (CHMeP), 12.2 (C_5Me_5). ^{31}P NMR (101 MHz, $CDCl_3$): δ −25.6 (s, PPh_2), −17.8 (s, PCy_2). Anal. Calcd for $C_{37}H_{46}P_2Ru$: C, 67.97; H, 7.09. Found: C, 67.92; H, 6.83.

Racemic (*S)-(*R**)-Cp*RuC$_5$H$_3$CH(Me){N$_2$C$_3$HMe$_2$-3,5)-PPh$_2$}-1,2 ((*S**)-(*R**)-11).** A pale yellow solution of (*S**)-(*R**)-**8** (0.60 g, 1.1 mmol) and 3,5-dimethylpyrazole (1.60 g, 16.6 mmol) in 5 mL of AcOH was heated at 60 °C for 30 min. Water (60 mL) was added, and the resulting suspension was made basic by careful addition of NaOH, followed by extraction with hexane (100 mL). The hexane extract was dried over $MgSO_4$ and the solvent removed *in vacuo*, leaving a crude product that was crystallized from ca. 50 mL of hot EtOH/H_2O (4:1) to give 0.32 g (49%) of pale yellow product.

(*S*)-(*R*)-Cp*RuC$_5$H$_3$CH(Me){N$_2$C$_3$HMe$_2$-3,5)PPh$_2$}-1,2 ((*S*)-(*R*)-11). The procedure is the same as above, except that (*S*)-(*R*)-**8** (0.65 g, 1.2 mmol) and 3,5-dimethylpyrazole (0.90 g, 9.3 mmol) reacted to give 0.80 g of crude product, contaminated by excess dimethylpyrazole. The compound could be obtained analytically pure in ca. 10% yield by repeated crystallization from EtOH/H_2O. ^{1}H NMR (250 MHz, $CDCl_3$): δ 7.51 (m, 2H, PPh_2), 7.25 (m, 3H, PPh_2), 6.98 (q, 3H, PPh_2), 6.85 (t, 2H, PPh_2), 5.14 (dq, 1H, CHMeN, ^3J(H,H) = 6.8, ^4J(P,H) = 1.9), 4.99 (s, 1H, N_2C_3H), 4.73, 4.30, and 4.01 (m, 3H, C_5H_3), 2.12, 1.93 (s, 2 × 3H, $N_2C_3HMe_2$), 1.81 (s, 15H, C_5Me_5), 1.59 (d, 3H, CHMeN, ^3J(H,H) = 6.9). ^{13}C NMR (63 MHz, $CDCl_3$): δ 135.5−126.8 (nonquartenary C of PPh_2), 104.2 (p-C of C_3N_2), 85.5 (C_5Me_5), 76.0, 75.4 (nonquartenary C of C_5H_3), 51.3 (d, CHMeN, ^3J(P,H) = 7), 20.0, 13.7 ($N_2C_3HMe_2$), 11.4 (CHMeP, ^4J(P,H) = 9), 11.7 (C_5Me_5). ^{31}P NMR (101 MHz, $CDCl_3$): δ −26.5 (s, PPh_2). ($[\alpha]_D^{20}$ = +202 ($CHCl_3$, c = 0.19)). Anal. Calcd for $C_{34}H_{39}N_2PRu$: C, 67.20; H, 6.47; N, 4.61. Found: C, 67.24; H, 6.46; N, 4.45.

Racemic (*S)-(*R**)-[(Cp*FeC$_5$H$_3$(CH(Me)PCy$_2$)(PPh$_2$)-1,2)Pd(η^3-C$_3$H$_5$)]$^+$[OTf]$^-$ ((*S**)-(*R**)-12).** To a stirred solution of [PdCl(η^3-C_3H_5)]$_2$ (52 mg, 0.14 mmol) and (*S**)-(*R**)-Cp*FeC$_5$H$_3$(CH(Me)PCy$_2$)(PPh$_2$)-1,2 (199 mg, 0.30 mmol) in CH_2Cl_2 (10 mL) was added Ag[CF_3SO_3] (77 mg, 0.30 mmol), dissolved in 1 mL of MeOH. After 1 h, the resulting brown suspension was filtered over Celite and the filtrate evaporated *in vacuo*. The orange spongy residue was dissolved in 10 mL of CH_2Cl_2 and layered with 50 mL of hexane. From this system, 210 mg (70%) of crystalline red product could be obtained overnight. ^{31}P NMR (101 MHz, $CDCl_3$): 2 isomers in approximate 1:2 ratio; minor isomer, δ 61.1 (d, PPh_2, ^4J(P,P) = 49 Hz), 17.0 (d, PCy_2, ^4J(P,P) = 49 Hz); major isomer, δ 58.7 (d, PPh_2, ^4J(P,P) = 46 Hz), 15.0 (d, PCy_2, ^4J(P,P) = 46 Hz). The ^{1}H and ^{13}C NMR spectra were poorly resolved indicating fluxionality in solution. Anal. Calcd for $C_{45}H_{59}O_3F_3P_2FePdS\cdot{}^1/_2CH_2Cl_2$: C, 54.48; H, 6.03. Found: C, 54.24; H, 5.91.

(*S)-(*R**)-[(Cp*RuC$_5$H$_3$(CH(Me)PCy$_2$)(PPh$_2$)-1,2)Pd(η^3-C$_3$H$_5$)]$^+$[OTf]$^-$ ((*S**)-(*R**)-13).** The procedure is the same as that for (*S**)-(*R**)-**12** except that [PdCl(η^3-C_3H_5)]$_2$ (24 mg, 0.07 mmol), (*S**)-(*R**)-**9** (100 mg, 0.14 mmol) in CH_2Cl_2 (5 mL), and Ag[CF_3SO_3] (36 mg, 0.14 mmol) reacted to give ca. 70 mg (50%) of crystalline product. ^{31}P NMR (101 MHz, $CDCl_3$): 2 isomers in approximate 2:3 ratio; minor isomer, δ 64.9 (d, PPh_2, ^4J(P,P) = 47 Hz), 14.4 (d, PCy_2, ^4J(P,P) = 47 Hz); major isomer, δ 67.8 (d, PPh_2, ^4J(P,P) = 47 Hz), 15.8 (d, PCy_2, ^4J(P,P) = 47 Hz). Anal. Calcd for $C_{45}H_{59}O_3F_3P_2RuPdS$: C, 53.70; H, 5.91. Found: C, 53.83; H, 6.09.

X-Ray Crystallographic Studies of 5, 9, 10, 12, and 13. Selected crystallographic and relevant data collection parameters for **9**, **12**, and **13** are listed in Table 1. Data were measured with variable scan speed to ensure constant statistical precision on the collected intensities. One standard reflection was measured every 120 reflections; no significant variation was detected.

The structures were solved either by direct (**5**, **10**, **12**, **13**) or Patterson (**9**) methods and refined by full-matrix least-squares using anisotropic displacement parameters for all non-hydrogen atoms. The contribution of the hydrogen atoms in their idealized position (riding model with fixed isotropic U = 0.080 Å^2) was taken into account but not refined. All calculations were carried out by using the Siemens SHELXTL PLUS system.

Acknowledgment. This research was in part supported by the Swiss National Science Foundation, program CHiral2 (postdoctoral grants to H.C.L.A. and J.S.).

Supporting Information Available: Tables of crystal data and refinement details, complete atomic coordinates and U values, complete bond distances and angles, and anisotropic displacement coefficients for the non-carbon atoms for compounds **5**, **9**, **10**, **12**, and **13** and ORTEP views and atom-numbering schemes for compounds **9** and **10** (Figures S1 and S2) (52 pages). Ordering information is given on any current masthead page.

OM9508997